International Conference on Nuclear Data for Science and Technology 2007
DOI: 10.1051/ndata:07326

Calculation of radionuclide production cross sections with FLUKA and their application in high energy hadron collider studies

M. Brugger[1,a], A. Ferrari[1], S. Roesler[1], and P.R. Sala[2]

[1] CERN, 1211 Geneva 23, Switzerland
[2] INFN Sezione de Milano, Via Celoria 16, 20133 Milano, Italy

Abstract. An overview is given of the models implemented in FLUKA which describe the production of radionuclides. Cross sections are calculated for hadron-induced reactions on materials used in the construction of accelerators from threshold up to energies of several TeV. The results form a database which is validated against experimental data. Dedicated activation measurements performed at an high-energy hadron accelerator complement the verification and confirm the accuracy of the FLUKA predictions. Finally, the importance of such a database is underlined with examples from radiological studies performed for the Large Hadron Collider (LHC).

1 Introduction

All stages in the life-cycle of a high energy accelerator require calculations of induced radioactivity. During the construction phase their results enter the design of components, the choice of materials as well as environmental impact studies. During operation they provide dose estimates for work on activated components and also the de-commissioning of an accelerator is based on studies of the nuclide inventory. For accelerators reaching TeV energies, Monte Carlo models used for such calculations must be able to reliably predict nuclide production in arbitrary target elements and at energies ranging from that of thermal neutrons to several TeV. For this reason, most studies for the Large LHC employ the Monte Carlo code FLUKA [1,2] which was found to be an appropriate Monte Carlo code for estimations of induced radioactivity at this accelerator [3].

In FLUKA induced radioactivity can be calculated directly by simulating the particle cascade in the respective components. However, this is not always the most efficient way to achieve results. Examples for such situations include materials of low density (e.g., air) or material compositions containing trace elements leading to the production of important nuclides, both cases for which obtaining results with low statistical uncertainty may imply significant CPU-time if nuclides are calculated directly. Similarly, it is not always efficient to re-run the entire simulation if details in the geometry or certain aspects in the nuclide production models have changed. In these situations it is often more appropriate to calculate particle fluence spectra in the regions of interest and fold them off-line with pre-computed, energy-dependent nuclide production cross sections.

This paper summarizes the main features of the models implemented in FLUKA used for predicting radionuclide production cross sections with emphasis to recent model improvements. Cross sections are calculated in a comprehensive way according to their relevance for radiological studies for the LHC and are compared to experimental data. The determination and convenience of such a data base is discussed with examples from radiological studies for the LHC.

[a] Presenting author, e-mail: Markus.Brugger@cern.ch

2 Radionuclide production in FLUKA

Residual nuclei (and, thus, radionuclides) in FLUKA emerge directly from the inelastic hadronic interaction models. With the exception of low-energy neutron interactions ($E < 19.6$ MeV), where tabulated data are used, radionuclide production cross sections can therefore be calculated with FLUKA for arbitrary projectile-target configurations (including nucleus-nucleus interactions) and energies. While this feature allows predictions for a large variety of applications the careful validation of radionuclide production with experimental data is of particular importance.

Nuclear interactions in FLUKA are simulated by PEANUT [4,5], a code which includes not only hadron scattering off nuclei but also the nuclear models for real and virtual photonuclear reactions, neutrino interactions, nucleon decays and muon captures. A major, recent improvement of PEANUT is the extension to TeV energies, which so far were modelled in FLUKA by separate modules [6]. In particular, the latter modules used a simplified implementation of intranuclear cascades in interactions at energies above 5 GeV which has now become obsolete. Only hadron-nucleus interactions beyond 20 TeV and nucleus-nucleus collisions involve independent codes (DPMJET [7], RQMD [8], BME [9]). However, all are coupled to PEANUT for evaporation and fragment de-excitation.

In PEANUT, hadron-hadron collisions are the main building blocks of hadron-nucleus collisions. Below a few GeV such interactions are simulated by the isobar model, through resonance production and decay, and by taking into account elastic, charge and strangeness exchange. At higher energies multiple collisions of each hadron with the nuclear constituents become important and are taken into account by means of the Glauber-Gribov calculus [10]. The implementation of elementary high-energy hadron-hadron collisions follows the Dual Parton Model (DPM) [11], coupled to a hadronization scheme. This model successfully describes so-called soft collision processes that cannot be addressed by perturbative QCD. At present, the implemented Glauber-Gribov formalism is being extended to return separately also the cross sections for quasi-elastic collisions (elastic scattering

of the projectile hadron off individual nucleons with subsequent decay of the target nucleus) such that these interactions can be consistently included in the particle production.

The high energy interactions are embedded into a sophisticated modelling of the propagation of produced hadrons and of associated nuclear effects. The description includes a generalized intra-nuclear cascade (GINC) with smooth transition to a pre-equilibrium stage performed with standard assumptions on exciton number or excitation energy. The GINC implementation in PEANUT adopts different nuclear densities for neutrons and protons, locally defined Fermi motion including wave packet-like uncertainty smearing and the curvature of particle trajectories due to the nuclear potential. Detailed mass tables supply the binding energies which are updated after each particle emission. The modelling also includes energy-momentum conservation and the computation of the recoil of the residual nucleus. Quantum effects are explicitly treated, among others, Pauli blocking, formation zone, nucleon anti-symmetrization, nucleon-nucleon hard-core correlations and coherence length. Nuclear medium effects on the Δ resonance properties are accounted for when treating pion interactions and pion re-interactions in the nucleus.

The GINC step of a nuclear interaction is followed by a pre-equilibrium stage. It describes the nuclear de-excitation as soon as all nucleons have reached energies below a smooth threshold energy of about 50 MeV, and all particles but nucleons (typically pions) have been emitted or absorbed. The input configuration for the pre-equilibrium stage is characterized by the total number of protons and neutrons, by the number of particle-like excitons (nucleons excited above the Fermi level), and of hole-like excitons (holes created in the Fermi sea by the INC interactions) as well as by the nucleus excitation energy and its momentum. All the above quantities are derived from the INC stage of the collision. The pre-equilibrium modelling is described in detail in ref. [12].

Emission of energetic light fragments through the coalescence process is included all along the PEANUT reaction chain. This allows also to reproduce the high energy tail of the light fragment spectra.

The final steps of the reaction include evaporation in competition with fission and gamma de-excitation. For light nuclei, a Fermi break-up model is implemented. The evaporation model, which is based on the Weisskopf-Ewing approach, has been continuously updated along the years, with the inclusion, for instance, of sub-barrier emission, full level density formula, analytic solution of the emission widths and evaporation of nuclear fragments up to $A \leq 24$. The accurate description of these processes is critical for a correct calculation of radioisotope production cross sections, as well as for the production of most neutrons. Recent improvements in the treatment of fission and in the adopted level densities were particularly effective for the description of residual nuclei production from heavy targets.

3 Cross section database and validation with experimental data

Radionuclide production cross sections were calculated with a non-standard FLUKA routine. It calls directly PEANUT for a given combination of projectile, target nucleus and energy and allows scoring of individual residual nuclei. As the routine also returns inelastic scattering cross sections, the cross sections for an individual radionuclide production channel follows directly from the probability of creating the nuclide in a collision. Since experimental cross sections are often reported based on cumulative yields the routine can optionally include unstable short-lived parent nuclide production into the calculated cross sections.

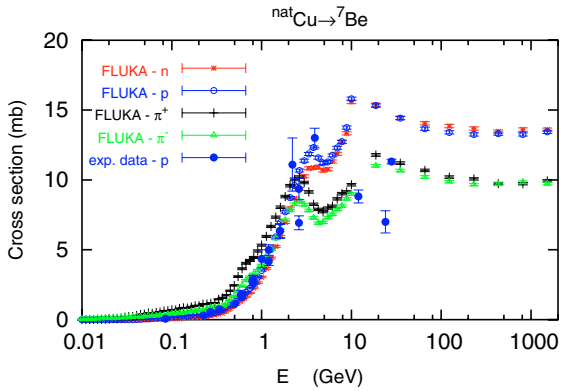

Fig. 1. Cross sections predicted by FLUKA for the production of ^{7}Be on natural copper by interactions of protons, neutrons and charged pions as function of energy. In addition, experimental data for proton-induced reactions are shown [13].

Since proton-, neutron- and charged pion-induced interactions dominate activation at high-energy hadron accelerators the database contains reaction cross section only for these four particle types. If needed for a certain application, it can however be extended at any time to other projectile types. Furthermore, the database is comprehensive for reactions on target nuclei with masses up to the one of zinc and includes cross sections for interactions on heavier targets only for selected masses. Considered energies range from threshold up to 10 TeV. In case of neutrons, the lower energy limit for the PEANUT calculation is 19.6 MeV, below which pretabulated cross sections are used. The Monte Carlo calculation consists of calls to PEANUT for a pre-defined energy binning (equidistant bins on a logarithmic scale), the number of calls at each energy being determined by the requirement to keep statistical uncertainties for individual nuclides below a few percent.

In total 103 isotopes were studied (^{3}H up to ^{72}Zn) produced by protons, neutrons and charged pions on 46 different target materials using their natural isotopic composition. Both non-cumulative and cumulative cross sections were calculated, with the latter containing all contributions from parent nuclides decaying via positive or negative beta decay and having a half-life smaller than the one of the respective isotope of concern. All cross section data base on the new PEANUT version (i.e., extended to all energies), which is expected to improve the reliability of FLUKA predictions as compared to previous versions used as, e.g., in the radionuclide production benchmark discussed in ref. [3]. Two examples are shown in figures 1 and 2.

The database has been validated with cross section data taken from literature as well as dedicated activation

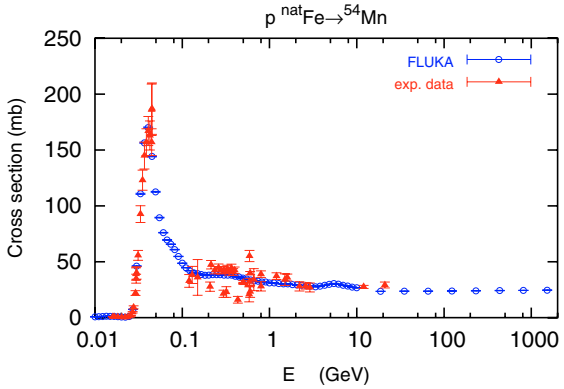

Fig. 2. Comparison of experimental cross sections [13] and FLUKA predictions for the production of ^{54}Mn on natural iron as function of energy.

benchmark measurements. ref. [13] contains the most comprehensive data collection and was used as main source of cross section data. Unfortunately, the data are not always consistent with each other and often scatter significantly, in particular at energies of a few GeV and above (for example, see fig. 1), an energy range which is important for many LHC-related applications. Therefore, dedicated irradiation experiments were performed over the past five years, to obtain additional experimental information on nuclide production by GeV-beams in materials typically used in the construction of the LHC accelerator (copper, iron, aluminum, titanium, etc.).

Results for material activation in the stray radiation field caused by a 120 GeV/c mixed hadron (35% protons, 61% positive pions, and 4% positive kaons) beam around a copper dump can be found in ref. [3] and references therein. Both specific activities and residual dose rates were measured and compared to detailed FLUKA simulations and remarkable agreement (within 20% for many nuclides) was found. In order to extend the experimental information to even higher energies where no or very scattered data exist an additional experiment was performed in the same irradiation facility (CERF) exposing iron and copper samples directly to the beam. The samples had a lateral size of 3 cm and a thickness of 0.5 cm (iron) and 1.1 cm (copper), respectively. After the exposure specific activities were measured at different cooling times by gamma spectrometry. Furthermore, the irradiation experiment was simulated with FLUKA and the specific activities calculated for the cooling times of the measurements. Tables 1 and 2 give the ratios of calculated and measured specific activities, along with the contribution to the production of each nuclide by interactions of beam particles as obtained with FLUKA. The last column in each table reports the ratios of calculated and measured specific activities of the previous experiment [3].

Due to the thicknesses of the samples beam particle interactions are responsible for only a fraction of the produced activity while the remaining part is produced in re-interactions of secondary particles. If the contribution by beam particle interactions is significant, as in case of ^{7}Be, the benchmark measurements directly yield the cross section at 120 GeV/c (cross section predicted by FLUKA divided with the given ratio). In all other cases, a cross section could be extracted, although with much higher uncertainties, taking into account

Table 1. Ratios of calculated and measured specific activities in the iron sample. In addition, the contributions by beam particle interactions to the production of the respective isotopes are given as well as the ratios of calculated and measured specific activities from the previous experiment [3].

Isotope	$t_{1/2}$	FLUKA / Exp. (this work)	Beam (%)	FLUKA / Exp. [3]
^{7}Be	53.3d	1.08 ± 0.16	91.2	1.65 ± 0.22
^{24}Na	15.0h	0.54 ± 0.03	90.4	0.48 ± 0.02
^{28}Mg	20.9h	0.57 ± 0.18	91.2	0.23 ± 0.03
^{m34}Cl	32.0m	0.36 ± 0.08	80.2	0.91 ± 0.19
^{38}Cl	37.2m	0.53 ± 0.09	84.6	0.61 ± 0.08
^{39}Cl	55.6m	0.55 ± 0.09	86.0	0.64 ± 0.11
^{41}Ar	1.8h	0.45 ± 0.07	85.5	0.46 ± 0.05
^{42}K	12.4h	0.54 ± 0.06	79.7	0.83 ± 0.06
^{43}K	22.3h	0.64 ± 0.06	82.7	0.77 ± 0.05
^{43}Sc	3.9h	0.43 ± 0.06	71.6	1.01 ± 0.14
^{44}Sc	3.9h	0.45 ± 0.03	71.1	1.06 ± 0.06
^{m44}Sc	58.6h	0.49 ± 0.04	71.1	1.20 ± 0.09
^{46}Sc	83.8d	0.54 ± 0.04	72.2	0.86 ± 0.07
^{48}Sc	43.7h	0.88 ± 0.15	79.6	1.47 ± 0.10
^{48}V	16.0d	0.66 ± 0.04	61.7	1.45 ± 0.06
^{48}Cr	21.6h	0.78 ± 0.08	61.9	0.97 ± 0.07
^{49}Cr	42.3m	0.68 ± 0.05	58.7	1.24 ± 0.12
^{52}Mn	5.6d	0.73 ± 0.04	53.8	1.15 ± 0.04
^{m52}Mn	21.1m	0.44 ± 0.05	53.8	1.24 ± 0.09
^{54}Mn	312.1d	0.68 ± 0.04	58.4	1.01 ± 0.10
^{56}Mn	2.6h	0.93 ± 0.08	46.8	0.99 ± 0.05
^{52}Fe	8.3h	0.56 ± 0.08	65.1	1.09 ± 0.13
^{55}Co	17.5h	0.77 ± 0.12	5.5	0.76 ± 0.04
^{56}Co	77.3d	0.63 ± 0.07	0.4	1.15 ± 0.10

the results of the previous experiment, which indicates the quality of the FLUKA predictions for interactions not caused by beam particles. The present benchmark results show that FLUKA predicts consistently lower activities. This fact could point to a systematic uncertainty in the data normalization or simulated irradiation geometry. An offset in the beam-monitoring however can be excluded based on prompt dose measurements performed in parallel to our exposures. Furthermore, the lateral beam shape as well as the beam alignment could, if not precisely known, also introduce systematic errors, especially in the present case of in-beam activation. The related effect was studied by simulating the irradiation with a pencil beam rather than a Gaussian-shaped beam and was found to be about 30%. However, since the beam *is* of Gaussian shape the deviation between the actual and assumed widths of the distribution is smaller and can also not fully account for the observed underestimation.

4 Applications

A cross section database has proven to be useful in three areas of application: parametric studies, activation of materials with

Table 2. As in table 1, here for the copper sample.

Isotope	$t_{1/2}$	FLUKA / Exp. (this work)	Beam (%)	FLUKA / Exp. [3]
^{7}Be	53.3d	0.94 ± 0.10	83.3	1.47 ± 0.19
^{24}Na	15.0h	0.58 ± 0.03	83.3	0.42 ± 0.03
^{28}Mg	20.9h	0.67 ± 0.06	84.2	0.25 ± 0.04
^{38}Cl	37.2m	0.48 ± 0.05	75.2	
^{39}Cl	55.6m	0.64 ± 0.08	78.0	
^{41}Ar	1.8h	0.47 ± 0.04	76.1	0.39 ± 0.06
^{42}K	12.4h	0.48 ± 0.05	71.1	0.66 ± 0.10
^{43}K	22.3h	0.64 ± 0.04	73.1	0.81 ± 0.10
^{43}Sc	3.9h	0.23 ± 0.03	64.1	0.40 ± 0.07
^{m44}Sc	58.6h	0.34 ± 0.03	64.2	
^{46}Sc	83.8d	0.52 ± 0.03	64.8	0.81 ± 0.07
^{48}Sc	43.7h	0.80 ± 0.07	68.8	1.39 ± 0.16
^{48}V	16.0d	0.52 ± 0.03	57.4	1.16 ± 0.08
^{48}Cr	21.6h	0.63 ± 0.10	56.9	0.92 ± 0.14
^{49}Cr	42.3m	0.52 ± 0.07	54.8	1.00 ± 0.22
^{52}Mn	5.6d	0.38 ± 0.02	48.8	0.68 ± 0.05
^{m52}Mn	21.1m	0.60 ± 0.09	48.8	
^{54}Mn	312.1d	0.56 ± 0.03	46.4	1.13 ± 0.12
^{56}Mn	2.6h	0.62 ± 0.04	52.7	0.81 ± 0.06
^{55}Co	17.5h	0.66 ± 0.06	41.0	0.66 ± 0.09
^{56}Co	77.3d	0.72 ± 0.04	37.6	1.04 ± 0.08
^{57}Co	271.8d	0.46 ± 0.03	35.6	0.85 ± 0.09
^{58}Co	70.8d	0.52 ± 0.03	35.4	0.91 ± 0.09
^{60}Co	5.3y	0.62 ± 0.06	48.8	0.90 ± 0.08
^{61}Co	99.0m	0.64 ± 0.04	59.5	0.68 ± 0.08
^{57}Ni	35.6h	1.02 ± 0.10	34.4	0.76 ± 0.11
^{65}Ni	2.52h	1.08 ± 0.20	0.3	1.46 ± 0.29
^{59}Fe	44.5d	0.63 ± 0.05	61.6	0.82 ± 0.09
^{60}Cu	23.7m	0.57 ± 0.06	30.4	0.78 ± 0.08
^{61}Cu	3.3h	0.79 ± 0.13	37.9	0.87 ± 0.25
^{64}Cu	12.7h	0.79 ± 0.08	49.6	0.63 ± 0.10
^{62}Zn	9.2h	0.57 ± 0.10	5.8	1.05 ± 0.23
^{65}Zn	244.3d	0.32 ± 0.05	0.2	0.62 ± 0.08

low (partial) density and model validation and development. Only a brief overview can be given in the following.

Radioactive waste calculations constitute an important example for parametric studies. The required accuracy (order of magnitude) often does not justify detailed and realistic simulations while approximate results are needed for all accelerator components which could possibly be activated, including the evaluation of different material choices. Related studies usually proceed by calculating typical energy spectra in simplified geometries containing only those components which may significantly alter the radiation field. The spectra are then folded offline with nuclide production cross sections of the materials in question to obtain a so-called nuclide vector. If more reliable cross sections become available or different materials are finally chosen for certain components the vector can easily be re-calculated by repeating the folding procedure.

A direct calculation of radionuclide production in gases or liquids (e.g., air or cooling water) or on trace elements in solid materials is often too time-consuming due to the low probabilities of the associated processes in the cascade simulation. Alternatively, particle energy spectra are calculated and folded with nuclide production cross sections. In case of environmental studies the latter are typically evaluated data providing upper estimates for the production cross sections in order to stay conservative in the water- or air-release estimates.

Finally, energy-dependent reaction cross sections allow detailed comparisons with experimental data (such as the data compilation of ref. [13]) and with predictions of other models. They provide far deeper insight into certain features of data and models than specific activities as the latter are integrated quantities, i.e., weighted with the fluence spectra at the location of interest. Also model improvements can be most easily appreciated if energy-dependent cross sections are compared.

References

1. A. Ferrari, P.R. Sala, A. Fassò, J. Ranft, CERN 2005-10 (2005), INFN/TC_05/11, SLAC-R-773 (2005).
2. A. Fassò et al., in *Proceedings of the International Conference on Computing in High Energy and Nuclear Physics, 2003 (CHEP2003), La Jolla, CA, USA, March 24–28, 2003* (paper MOMT005) eConf C0303241 (2003), arXiv:hep-ph/0306267.
3. M. Brugger, A. Ferrari, S. Roesler, L. Ulrici, Nucl. Instrum. Meth. Phys. Res. Section A **562**, 814 (2006).
4. A. Ferrari, P.R. Sala, in *Proceedings of the International Conference on Monte Carlo Simulation in High-Energy and Nuclear Physics, MC93* (World Scientific, 1994), p. 277.
5. A. Fassò, A. Ferrari, J. Ranft, P.R. Sala, in *Proceedings of the Specialists' Meeting on Shielding Aspects of Accelerators, Targets & Irradiation Facilities, Arlington, TX, USA, April 28–29, 1994* (OECD Documents, Paris, 1995), pp. 287–304.
6. G. Battistoni et al., in *Proceedings of the 11th International Conference on Nuclear Reaction Mechanisms*, Ric. Scient. ed Ed. Perm. Suppl., edited by E. Gadioli **126**, 483 (2006).
7. S. Roesler, R. Engel, J. Ranft, in *Proceedings of the Monte Carlo 2000 Conference, Lisbon, Portugal, Oct. 23–26, 2000*, edited by A. Kling, F. Barao, M. Nakagawa, L. Tavora, P. Vaz (Springer-Verlag, Berlin, 2001), pp. 1033–1038.
8. V. Andersen et al., Adv. Space Res. **34**, 1302 (2004).
9. F. Cerutti et al., J. Phys.: Conf. Ser. **41**, 212 (2006).
10. V.N. Gribov, Sov. Phys. JETP **29**, 483 (1969).
11. A. Capella, U. Sukhatme, C.-I. Tan, J. Tran Thanh Van, Phys. Rep. **236**, 225 (1994).
12. A. Ferrari, P.R. Sala, in *Proceedings of the Workshop on Nuclear Reaction Data and Nuclear Reactors Physics, Design and Safety*, edited by A. Gandini, G. Reffo **2**, 424 (1998).
13. Landolt-Börnstein, *Zahlenwerte und Funktionen aus Naturwissenschaften und Technik, Radionuklidproduction bei mittleren Energien* (Springer-Verlag, Bd. 13, 1991).